

Effects of photoelectric therapy on proliferation and apoptosis of scar cells by regulating the expression of microRNA-206 and its related mechanisms

Song Zhang | Zhen-Min Zhao  | Hong-Yu Xue | Fang-Fei Nie

Department of Plastic Surgery, Peking University Third Hospital, Beijing, China

Correspondence

Zhen-Min Zhao, Department of Plastic Surgery, Peking University Third Hospital, No. 49 North Garden Road, Beijing, 100191, China.
Email: zhaozhenmin0098@vip.sina.com

Abstract

Human skin fibroblast (HSF) cells were irradiated with different energy lasers to detect cell proliferation, apoptosis, and expression of microRNA-206 and protein, and to further summarise the therapeutic effect of laser on scar cells. Human scar cell line HSF cells were cultured in three groups. The control group was not irradiated by laser, the low-energy group was irradiated by 10 J/cm² laser, and the high-energy group was irradiated by 20 J/cm² laser. After irradiation, HSF cells were cultured for 20 hours. Cell proliferation was detected by MTT assay. Cell cycle and apoptosis were detected by flow cytometry. Transwell migration assay was used to detect cell migratory ability. Reverse transcription polymerase chain reaction (RT-PCR) was used to detect miR-206 and *mTOR* gene levels. The levels of MMP-9, Bax, Bcl-2, cyclin D1, and mTOR signalling pathway proteins were detected by Western blotting assays. The results showed that after laser irradiation, the proliferation of cells decreased, and the difference between the control group and the experimental group was significant ($P < .05$). The higher the energy was, the greater the upregulation of apoptosis was. Apoptosis and cell migration increased ($P < .05$). The expressions of microRNA-206, MMP-9, and Bax were upregulated, while the expressions of mTOR, Bcl-2, and cyclin D1 were downregulated. To sum up, laser irradiation can significantly inhibit the proliferation of HSF cells, affect cell cycle, and increase cell apoptosis and migratory ability.

KEYWORDS

apoptosis, cell proliferation, laser, scar cells

1 | INTRODUCTION

Pathological scar (PS) is the result of abnormal repair of human skin after trauma. It mainly includes hypertrophic scar and keloid.¹ It is a kind of pathological repair with the imbalance of extracellular matrix synthesis and

decomposition caused by excessive proliferation of fibroblasts and large amount of collagen synthesis and disorder of collagen fibre arrangement, which are the main histological manifestations.²⁻⁴ PS mainly occurs secondary to burns, trauma, surgery, infection, and so on. At present, the clinical treatments for PS include surgical

excision, drug injection, pressure therapy, local radiotherapy, and photoelectric therapy, and so on. Among them, photoelectric therapy is gradually recognised and widely used clinically.

The principle of laser treatment of scar is to remove scar tissue or injure scar vessels, inhibit collagen synthesis and cell proliferation, and induce cell apoptosis by utilising the special functions of laser such as burning, gasification, cutting, coagulation, and defocusing. Different kinds of lasers have different wavelengths, different absorption groups, and different mechanisms. The main absorption groups of pulsed dye laser (PDL), adjustable pulse width Nd:YAG doubling laser (VPW532 nm/532 nm KTP), and long pulse width Nd:YAG 1064 nm laser are oxyhaemoglobin, which specifically damages blood vessels in scars, promotes heat coagulation and necrosis of vascular endothelial cells, inhibits vascular proliferation, aggravates tissue hypoxia, leads to collagenase release, and promotes the number of fibroblasts. When the amount of extracellular matrix (EXM) is decreased, the degradation of EXM is increased, thus inhibiting the growth of scar and promoting scar atrophy.⁵ Some scholars believe that 585/595 nm PDL can inhibit the expression of transforming growth factor-beta (TGF- β), upregulate the expression of matrix metalloproteinases (MMPs), and increase the apoptosis of fibroblasts, thus promoting scar shrinkage. It can stimulate the proliferation of mast cells, promote the release of histamine, combine with its thermal effect, and cause the remodelling of collagen fibres.^{6,7} The characteristic of 532 nm KTP is that the pulse width can be adjusted according to the thickness and depth of blood vessels. Some scholars have compared 532 nm KTP and 595 nm PDL in the treatment of erythematous scars within 24 months after operation. Both are equally safe and effective in the treatment of scars. KTP is superior to PDL in improving the distribution and quantity of blood vessels in scars, but the average pain score of KTP is higher than that of PDL in the treatment, which may be due to oxidised haemoglobin.⁸ The protein absorbs KTP more strongly. 532 nm KTP has the advantages of less heat damage, fewer adverse reactions such as purpura after operation, and short recovery period, but it still has the risk of erythema and oedema formation. In addition, it can competitively enhance the absorption of melanin and increase the potential risk of epidermal injury and pigmentation. Long pulse width Nd:YAG 1064 nm laser cannot only selectively inhibit the formation of microvessels in scars and induce atrophy or closure, but also selectively inhibit the synthesis of collagen and the expression of type I procollagen gene without affecting cell activity and DNA replication, so as to treat scars.^{9,10}

MicroRNA is a single-stranded, non-coding RNA containing 19–30 nucleotides that plays a role by

Key Messages

- pathological scar is the result of abnormal skin repair in humans after trauma. Laser treatment can inhibit collagen synthesis, cell proliferation, and induce apoptosis
- miR-206 is widely distributed in various tissues and cells. However, studies on the mechanism of miR-206 scar cell proliferation and apoptosis are not comprehensive and in-depth
- laser irradiation can reduce the proliferation of HSF cells and promote their ability to migrate
- laser irradiation increases the transcription of miR-206
- laser irradiation causes Bax, MMP-9, mTOR upregulation, and Bcl-2 downregulation

downregulating or inhibiting its translation. In 1993, Lee et al discovered lin-4, the first member of the short-chain non-coding RNA family, which opened a new era of non-coding RNA research. miR-206 was originally cloned and identified from human and mouse muscle tissues.¹¹ Its length was 22 nt. It was matured by shearing stem-ring precursors of 73 nt. Its coding gene was located on chromosome 6. It has been reported that miR-206 exists widely in various tissues and cells and participates in various biological functions.¹² For example, in renal cell carcinoma, endometrial adenocarcinoma, and ovarian cancer, upregulation of the expression of miR-206 can inhibit cell proliferation and migration.^{13–15} However, the study on the mechanism whereby miR-206 regulates scar cell proliferation and apoptosis is not comprehensive and in-depth.

This study first discussed the effects of miR-206 on the proliferation and apoptosis of scar cells and its related mechanisms in order to provide a new theoretical basis and research direction for photoelectric therapy of PS.

2 | MATERIALS AND METHODS

2.1 | Cell culture

Human scar cell line human skin fibroblast (HSF) cells were purchased from the Cell Bank of the Chinese Academy of Sciences (Shanghai, China). Cells were maintained in 5% CO₂ at 37°C with dulbecco's modified eagle medium (Grand Island, NY) containing 10% fetal

bovine serum (FBS) and antibiotics (Rockville, Maryland). The cells were inoculated into sterile 96-well plates at 37°C in an incubator (Thermo Fisher, 3100) containing 5% CO₂ air. Three groups were set up in the experiment. The control group was not irradiated by laser, the low energy group was irradiated by 10 J/cm² laser density, and the high energy group was irradiated by 20 J/cm² laser density. The cells were cultured for 20 hours.

2.2 | CCK8 assay for cell proliferation

Cell suspension was prepared and inoculated into 96-well plate at a density of 1×10^4 cells per hole. About 100 μ L cell suspension was added into each well. The experiment was performed in triplicates and the cells were cultured for 12 hours to adhere to the cell wall. The 10 μ L CCK-8 reagent was added into the cells and incubated for 1 hours at 37°C. The absorbance (*A*) values of all samples were read at 450 nm on a microplate reader (Thermo, Multiskan MK3, Waltham, MA). Cell inhibition ratio was calculated based on the following formula:

$$\text{Cell inhibition ratio (\%)} = (1 - A_{\text{experimental}}/A_{\text{control}}) \times 100\%.$$

2.3 | Detection of cell cycle and apoptosis by flow cytometry

Cells were seeded on plates for 12 hours and treated with 0.25% trypsin for 24 hours. Cells were washed three times with phosphate-buffered saline (PBS). Cell suspension evaluated for apoptosis through Annexin V-FITC (California). Cell cycle and apoptotic cells were detected by using a FACSCalibur flow cytometer (BD Biosciences, California).

2.4 | Transwell assays for cell migration

Cells were harvested and then suspended in 200 μ L of serum-free media. For migration assays, 3×10^5 cells in serum-free medium were directly added into the upper chamber. For invasion assays, the melted Matrigel (BD Biosciences, San Jose, California) was diluted with culture medium; the chamber was incubated for 4 hours at 37°C in order to allow Matrigel to solidify and then 3×10^5 cells in serum-free medium were added into the upper chamber. Medium containing 20% FBS was added to the lower chamber and served as a chemoattractant. After incubation in an incubator for 24 hours under 37°C and 5% CO₂ conditions, the cells that migrated to or invaded the lower surface of the membrane were fixed

with 4% paraformaldehyde, stained in 10% crystal violet, and rinsed with PBS; these cells were counted under a microscope at high power in randomly selected fields in each chamber; and the number of computational units in each visual field is recorded. The number of cells passing through the membrane was counted under a microscope at a magnification of $\times 400$. Each experiment was performed in triplicate.

2.5 | Detection of microRNA-206 and mTOR gene levels by real-time PCR

Total cellular RNA was extracted using TRIzol Reagent (California). Expression of miR-206 and mTOR was quantified in human HSF cells by real-time PCR miRNA kit. Quantitative reverse transcription polymerase chain reaction (RT-PCR) was performed using the ABI Prism 7500 (Applied Biosystems). The fold change in expression was calculated according to the comparative Ct ($\Delta\Delta$ Ct) method. The primers of miR-206 and mTOR are as follows: miR-206 forward, 5'-CTCAACTGGTGTCTGGGA-3'; miR-206 reverse, 5'-TCGGCAGGTGGAATFTAAG-3'; mTOR forward, 5'-GCAGCTGAATCTACAGGGCATC-3'; and mTOR reverse, 5'-GTTTGT AGTGTAGCACAGCTTCG-3'. The incubation was initiated at 37°C for 15 minutes, followed by 95°C for 5 minutes, 95°C for 10 seconds, 58°C for 20 seconds, 40 cycles at 95°C for 15 seconds, 65 °C for 1 minute, and 95 °C 15 seconds. The experiment was performed in triplicate three times independently.

2.6 | Detection of MMP-9, Bax, Bcl-2, cyclin D1, and mTOR protein level by Western blotting assays

Cells were washed three times with PBS and prechilled cell lysate was added to cells. Then, the solution was fully mixed and put on ice for 20 minutes, followed by centrifugation at $12000 \times g$ for 20 minutes. The proteins were blocked with 5% skim milk overnight at 4°C after transfer to membrane. After washing with Tris-buffered saline three times, the membranes were incubated in anti-MMP-9 (Abcam, AB76003, 1:1000), anti-Bax (Proteintech, 50599-21g, 1:1000), anti-Bcl-2 (Abcam, AB218123, 1:1000), anti-cyclin D1 (Beyotime, AF0126, 1:1000), and anti-mTOR antibodies (Cell Signaling, 2983S, 1:1000) at 37°C for 1 hour. Then, the protein bands were visualised using ECL reagents, and images were captured using the ChemiDoc Imaging system. Western blotting assays were performed at least three times independently.

3 | RESULTS

3.1 | Effect of laser irradiation on proliferation of HSF cells

The results are shown in Figure 1. Laser irradiation can reduce the cell proliferative ability. The control group

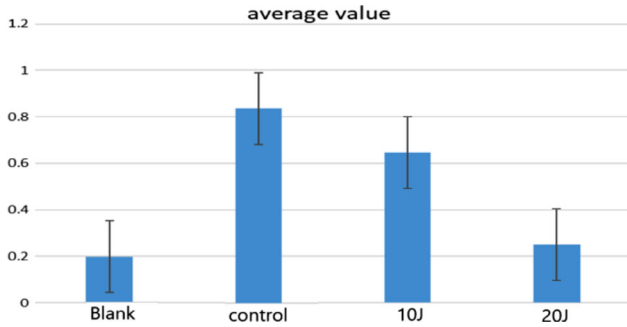


FIGURE 1 Mean value of HSF cell proliferation ability by CCK8 assays

without laser irradiation showed the strongest cell proliferation ability (0.836), while the high-energy irradiation (20 J/cm²) had the slowest (0.25). There was a significant difference among the three groups ($P < .05$).

3.2 | Effect of laser irradiation on HSF cell cycle progression

Flow cytometry showed that the ratio of G1 phase cells to total cells irradiated by laser was significantly higher than that of the control group ($P < .05$), and from the peak figure control group, G2/M phase blockade, that is, DNA synthesis increased, cell proliferation was promoted (Figure 2).

3.3 | Effect of laser irradiation on HSF cell apoptosis

The apoptotic rates of different treatment methods were as follows (Figure 3): the control group (1.58%)

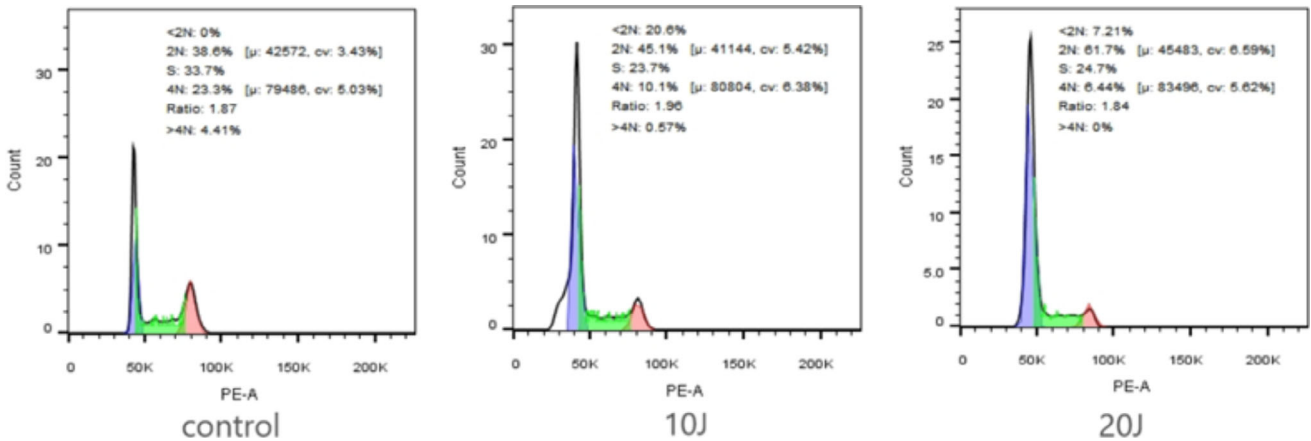


FIGURE 2 Cycle contrast map of HSF cells detected by flow cytometry

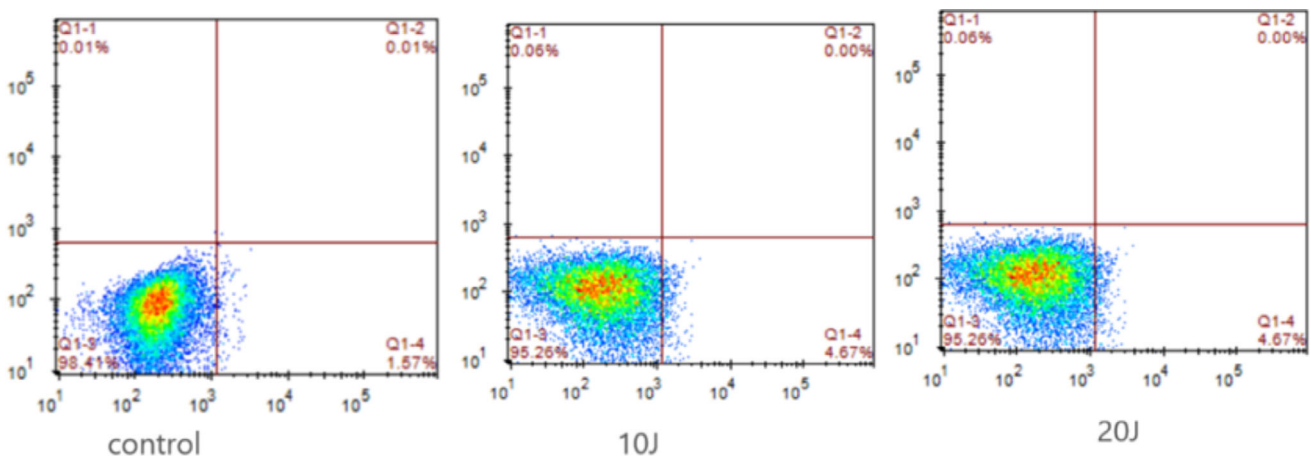


FIGURE 3 Apoptotic results of the three groups

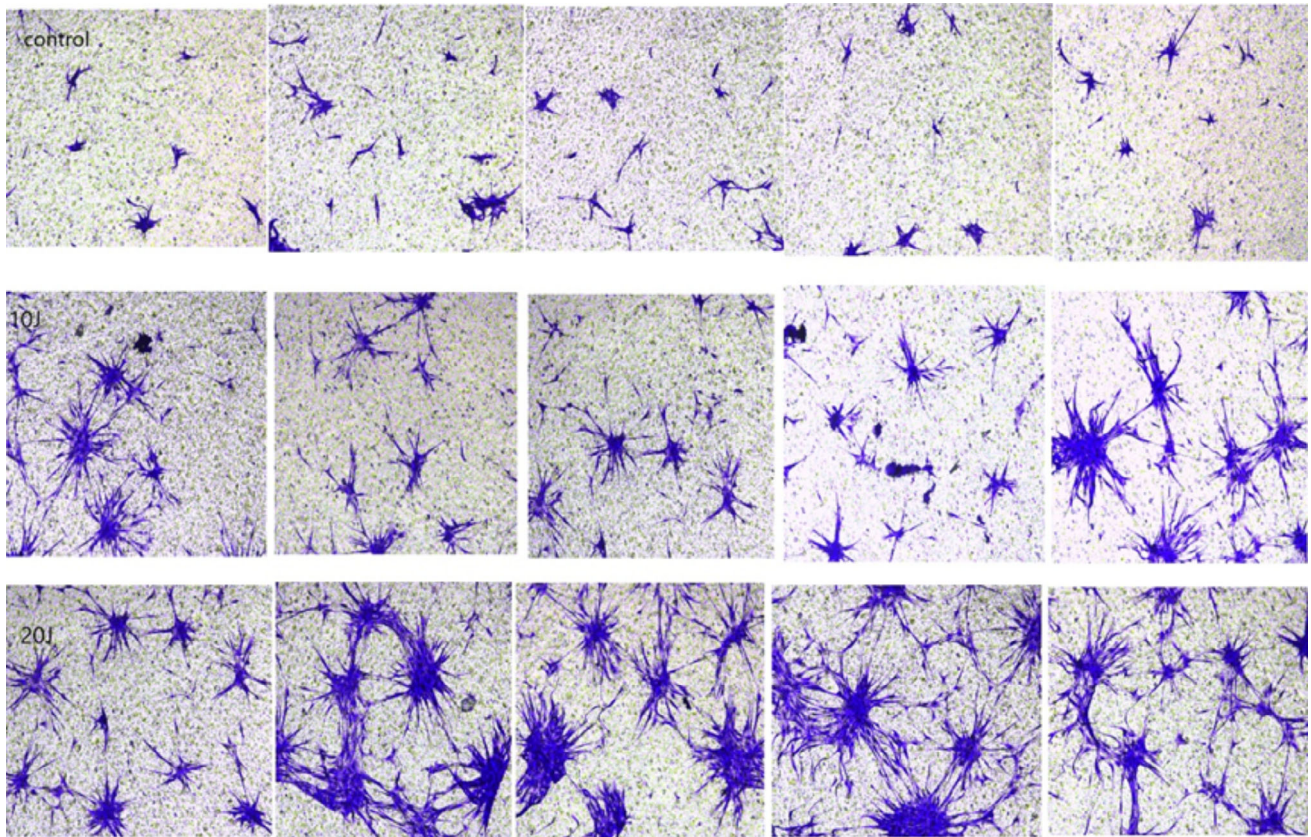


FIGURE 4 Contrast map of HSF cell migration ability

< the low-energy group (4.67%) < the high-energy group (5.58%), and there were significant differences between the control group and the experimental group ($P < .05$). So the higher the energy was, the greater the upregulation of apoptosis was and the weaker the increment ability was.

3.4 | Effect of laser irradiation on HSF cell migration

The results are shown in Figure 4. The migratory ability of cells improved after laser irradiation. In a certain range, the migratory ability of cells in the high-energy group was the highest.

3.5 | Effect of laser irradiation on the expression of miR-206 and mTOR

The results of qPCR showed that the mean CT value of *mTOR* in the non-laser irradiation group was 33.94, that of the low-energy laser irradiation group (10 J/cm²) was 33.45, and that of the high-energy laser irradiation group (20 J/cm²) was 33.55. The CT values of three genes (one internal reference gene and two target genes)

were not significantly different ($P > .05$) (Figure 5A). The mean CT values of *MIR-206* in the three groups were 22.33, 20.95, and 20.11, respectively. According to the formula for calculating the relative expression of each sample, as far as the relative expression of *mTOR* is concerned, cells without laser irradiation showed the highest expression,¹ cells irradiated by high-energy laser had the lowest expression (0.56), and the expression in cells irradiated by low-energy laser was 0.83 (Figure 5B). In contrast, the relative expression of *miR-206* was the lowest in non-laser irradiated samples.¹ With the increase of laser energy, the relative expression of *miR-206* increased. The relative expression of *miR-206* in the high-energy laser irradiated group was 2.01 (Figure 5C).

3.6 | Effect of laser irradiation on the expression of MMP-9, Bax, Bcl-2, cyclin D1, and mTOR signalling proteins

The protein concentration of the samples determined by bicinchoninic acid was 1.642 mg/mL in the blank control group, 5.413 mg/mL in the low-energy group, and 1.874 mg/mL in the high-energy group. The integrated

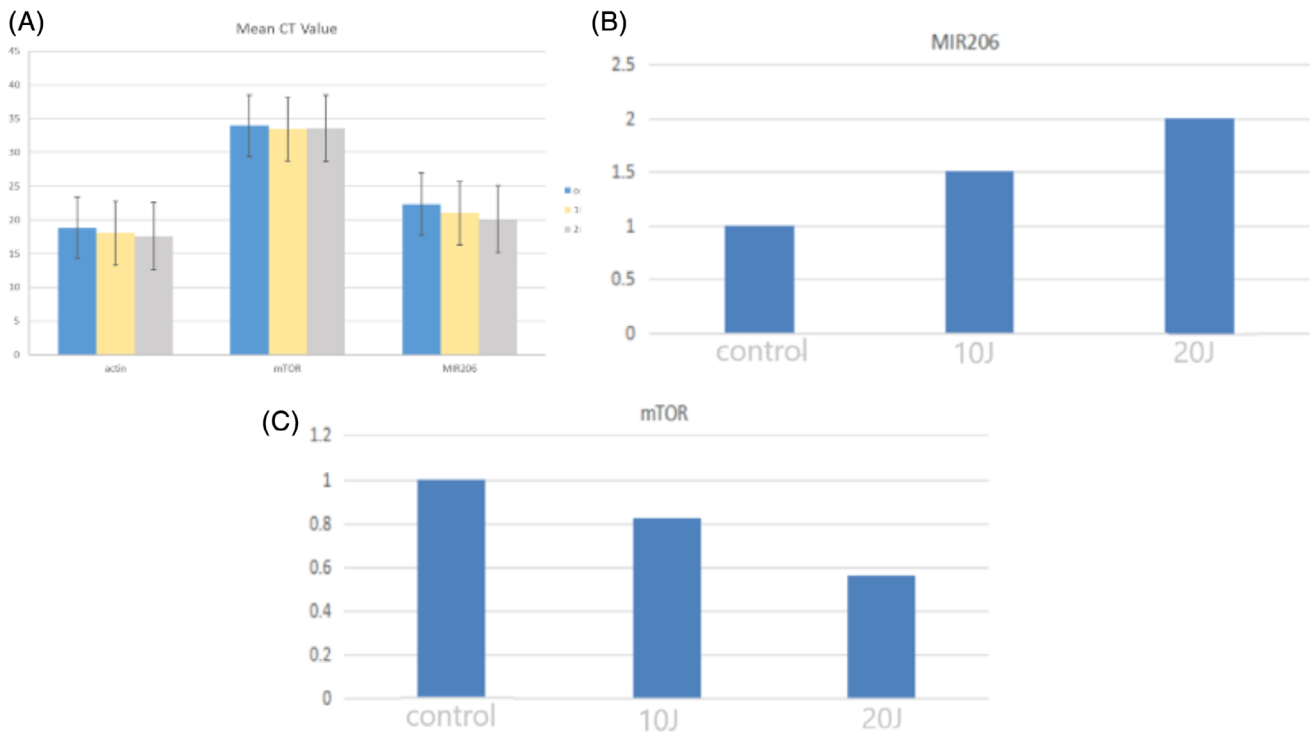


FIGURE 5 Mean CT values and relative expression of *miR-206* and *mTOR* in the three groups

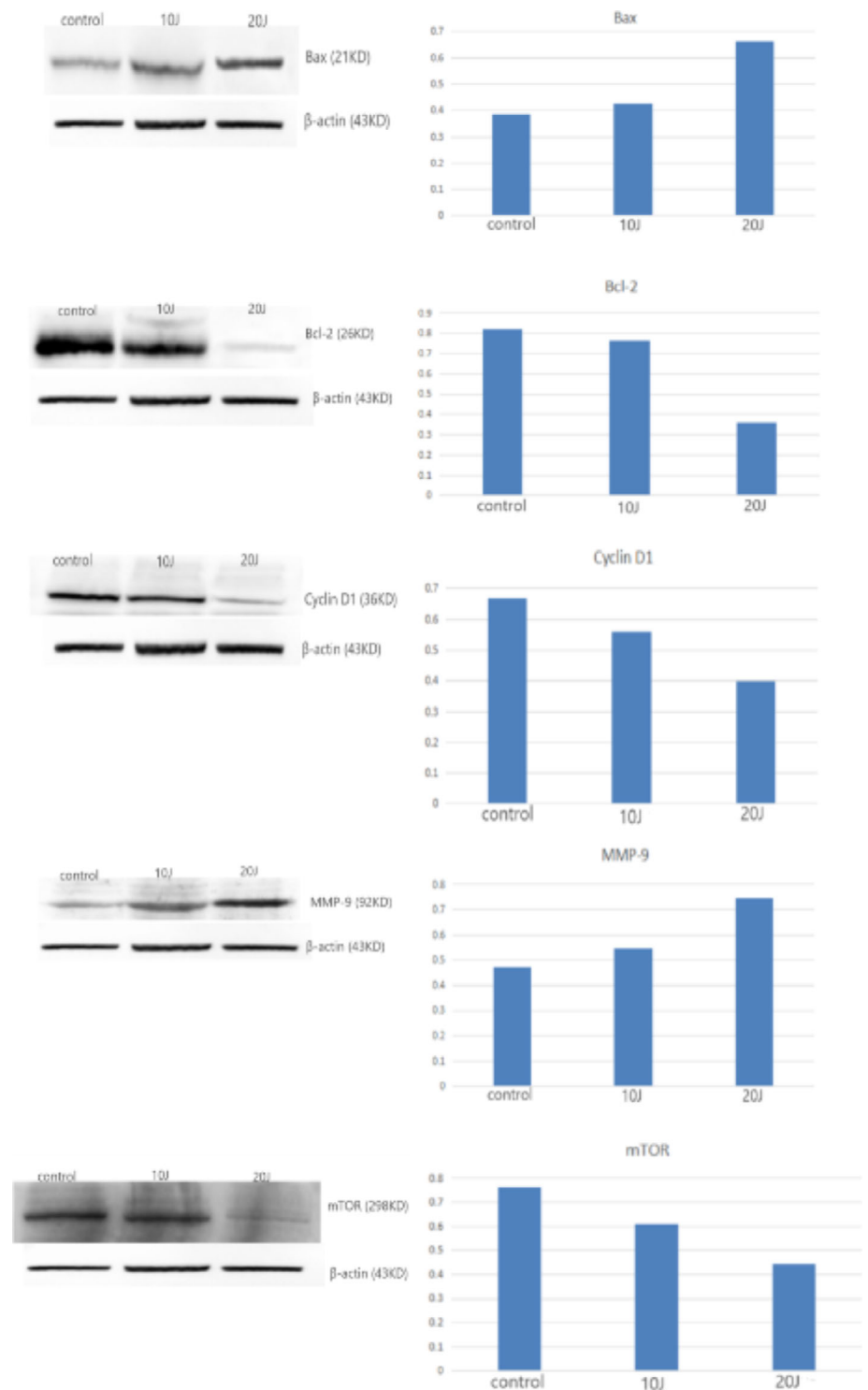
density of β -actin in the three groups was 230 807 in the blank control group, 310 409 in the low-energy group, and 262 093 in the high-energy group. The relative expression of the target protein in each sample was expressed by the grey value of the target protein/the grey value of the internal reference protein. The relative expression of *Bax* in the three groups was 0.386, 0.427, and 0.661, respectively, and the expression of *Bax* increased with the increase of energy of irradiated cells (Figure 6). In contrast, the expression of *Bcl-2* decreased with the increase of laser irradiation energy, 0.361 in the high-energy group, 0.763 in the low-energy group, and 0.819 in the control group (Figure 6). The relative expression of cyclin D1 was as follows: 0.669 in the control group, 0.559 in the low-energy group, and 0.398 in the high-energy group (Figure 6). The relative expression of *MMP-9* in the blank group, low-energy group, and high-energy group was 0.473, 0.546, and 0.743, respectively (Figure 6). The relative expression of *mTOR* in the three groups was 0.759, 0.610, and 0.443, respectively, and the expression of *mTOR* decreased with the increase of irradiation energy (Figure 6). In summary, laser irradiation has an effect on the relative expression of proteins in each sample. *Bcl-2* and cyclin D1 are downregulated, and the protein expression decreases with the increase of energy. *Bax*, *MMP-9*, and *mTOR* are upregulated, and the relative expression increases with the increase of energy.

4 | DISCUSSION

In this study, we irradiated HSF cells with high-energy and low-energy laser, respectively. The cells without laser irradiation were used as controls. Then, the proliferation and apoptosis of HSF cells were examined. The expression levels of *microRNA-206* and *mTOR* were detected by RT-PCR, and the expression level of protein was detected by Western blotting assays. The results showed that apoptosis was induced by irradiation, and the higher the energy was, the greater the apoptotic upregulation range was and the opposite the value-added ability. The stronger the irradiation energy was, the higher the expression of *microRNA-206*, *MMP-9*, and *Bax* protein was, and the lower the expression of *mTOR*, *Bcl-2* and cyclin D1 was.

Some studies have shown that laser can treat hypertrophic scars, but the specific mechanism of its action still needs further studies.^{16,17} The application of PDL in the treatment of scars began in the early 1990s. The principle is that PDL can specifically act on microvessels.¹⁸ The principle of PDL in scar treatment is to inhibit the formation of small blood vessels and close small blood vessels, so as to aggravate the degree of scar hypoxia and reduce the sources of growth factors and fibroblasts as well as to prevent and treat scars. Alster et al used a 585-nm flash-PDL to treat resting erythematous hypertrophic scars. Studies such as skin texture analysis and clinical observation confirmed that one to two times of treatment had

FIGURE 6 Relative expression of Bax, Bcl-2, cyclin D1, MMP-9, and mTOR in the three groups



marked improvement.^{19,20} The proliferation and activation of fibroblasts in hypertrophic scars are regulated by many cytokines, including TGF- β , fibroblast growth factor, connective tissue growth factor, interleukin-6, and epidermal growth factor.²⁻⁴ Among them, TGF- β 1 is a powerful chemokine and stimulant, which can stimulate fibroblast proliferation and aggravate scar growth. Some

studies have shown that a 595-nm PDL can effectively inhibit the secretion of TGF- β 1 and ultimately play a role in the treatment of scars.

Barak et al have demonstrated that laser irradiation induces apoptosis of human retinal pigment epithelial cells.²¹ They believed that the induction of apoptosis was accompanied by the increase of ceramide, which might

be the second messenger involved in apoptotic cascade reactions. Mesenchymal stem cells (MSCs) have been proved to be an important element in cell-based therapy. Photobiomodulation used extremely low-level lasers (LLs) to affect the behaviour of cells. The effect of LLs on human MSCs remained to be discovered. Yin et al studied the effect of LL on MSCs cultured in vitro. They found that with the increase of Bcl-2 and the decrease of bax, the resistance of LLs to apoptosis increased, suggesting that LLs can improve the survival rate and therapeutic function of stem cells, which may be a new pretreatment method for MSCs.²² This is similar to our experimental results. After laser irradiation, the expression of Bax protein is upregulated and Bcl-2 is downregulated.

Shu et al discussed the inhibition of a high-power He-Ne laser on scar growth after trauma.²³ in vitro experiments showed that the cell proliferation index decreased, and the percentage of G0/G1 phase cells increased in irradiation group. In animal study, the area exposed to He-Ne irradiation showed a significant reduction in scar thickness, hydroxyproline level, and PCNA protein expression. The results of in vitro and in vivo studies showed that repeated irradiation with He-Ne laser at a certain power density inhibited fibroblast proliferation and collagen synthesis, thereby inhibiting the growth of hypertrophic scars. Our results also showed that cell proliferation was slowed down after laser irradiation.

MMPs belong to the metal-dependent endopeptidase family, of which MMP-9 is an important member. MMP-9 can degrade the extracellular matrix and enhance the motility of epithelial cells. Esquenazi's study showed that changes in collagen composition and the presence of MMP-9 at the wound margin over several years after laser-assisted in situ keratomileusis indicated active wound remodelling.²⁴

Cyclin D1 promotes cell proliferation. It binds to and activates cyclin-dependent kinase CDK4 specific to the G1 phase. Cyclin D1 phosphorylates cyclin inhibitor protein (Rb) in the G1 phase. Phosphorylated Rb dissociates from its binding with the E2F transcription factor, which then initiates the transcription of cell cycle associated genes. As a result, the cell cycle is promoted from G1 to S. From our experimental results, we can see that after laser irradiation, the protein expression is downregulated, which further indicates that cell proliferation is inhibited, which is consistent with the results measured by MTT method.

More and more evidence showed that miR-206 can significantly inhibit chondrocyte proliferation and promote cell apoptosis. RT-PCR results show that the expression of microRNA-206 is significantly higher than that of

control group, that is, the apoptosis of the experimental group is higher than that of the control group.

The mTOR pathway incorporates both intra- and extracellular signals. It is also an important regulator of many physiological processes such as growth, metabolism, proliferation, metastasis, and malignant transformation of human tumours. It has been proved that high-dose laser irradiation (0.8 J)/cm² can significantly reduce the expression of mTOR protein.

5 | CONCLUSIONS

In conclusion, high-energy laser can inhibit cell proliferation and promote cell apoptosis, which has a positive effect on the treatment of scar cells. Our experiment may also have some limitations as only two gradients were selected for comparison, so the amount of data is less. The formation and treatment of hypertrophic scar are influenced by many factors. Because of the network characteristics of various cytokines, the biological activities interact with one another, and there are differences between in vivo and in vitro experiments. It is necessary to further study the effects of other laser cytokines, microvessels, and fibroblasts.

CONFLICT OF INTEREST

The authors declare no potential conflict of interest.

ORCID

Zhen-Min Zhao  <https://orcid.org/0000-0002-1483-4861>

REFERENCES

1. Tu L, Huang Q, Fu S, Liu D. Aberrantly expressed long non-coding RNAs in hypertrophic scar fibroblasts in vitro: a microarray study. *Int J Mol Med*. 2018;41(4):1917-1930.
2. Mohammad G, Mamiko T, Hajime S, Hiko H, Oichi K. Functional implications of the IL-6 signaling pathway in keloid pathogenesis. *J Invest Dermatol*. 2007;127(1):98.
3. Grieb G, Steffens G, Pallua N, Bernhagen J, Bucala R. Chapter one-circulating Fibrocytes-biology and mechanisms in wound healing and scar formation. *Int Rev Cell Mol Biol*. 2011; 291:1-19.
4. Rhett JM, Ghatnekar GS, Palatinus JA, O'Quinn M, Yost MJ, Gourdie RG. Novel therapies for scar reduction and regenerative healing of skin wounds. *Trends Biotechnol*. 2008;26(4): 173-180.
5. Anderson RR, Donelan MB, Hivnor C, et al. Laser treatment of traumatic scars with an emphasis on ablative fractional laser resurfacing: consensus report. *JAMA Dermatol*. 2014;150(2):187-193.
6. Kuo YR, Wu WS, Wang FS, Huang HC, Lin CZ, Yang KD. Suppressed TGF-beta1 expression is correlated with up-regulation of matrix metalloproteinase-13 in keloid regression

- after flashlamp pulsed-dye laser treatment. *Lasers Surg Med.* 2005;36(1):38-42.
7. Brewin MP, Lister TS. Prevention or treatment of hypertrophic burn scarring: a review of when and how to treat with the pulsed dye laser. *Burns.* 2014;40(5):797-804.
 8. Keane TC, Tanzi E, Alster T. Comparison of 532 nm potassium Titanyl phosphate laser and 595 nm pulsed dye laser in the treatment of erythematous surgical scars: a randomized, controlled, open-label study. *Dermatol Surg.* 2015;42(1):70.
 9. Elsaie ML, Choudhary S, Mcleod M, Nouri K. Nd: YAG laser treatment for keloids and hypertrophic scars: an analysis of 102 cases: erratum. *Plast Reconstr Surg.* 2015;3(4):1.
 10. Al-Mohamady EH, Ibrahim SMA, Muhammad MM. Pulsed dye laser versus long-pulsed Nd:YAG laser in the treatment of hypertrophic scars and keloid: a comparative randomized split-scar trial. *J Cosmet Laser Ther.* 2016;18(4):208-212.
 11. Hak Kyun K, Sun LY, Umasundari S, Ankit M, Anindya D. Muscle-specific microRNA miR-206 promotes muscle differentiation. *J Cell Biol.* 2006;174(5):677-687.
 12. Liu F, Zhao X, Qian Y, Zhang J, Zhang Y, Yin R. MiR-206 inhibits head and neck squamous cell carcinoma cell progression by targeting HDAC6 via PTEN/AKT/mTOR pathway. *Biomed Pharmacother.* 2017;96:229-237.
 13. Xiao H, Xiao W, Cao J, et al. miR-206 functions as a novel cell cycle regulator and tumor suppressor in clear-cell renal cell carcinoma. *Cancer Lett.* 2016;374(1):107-116.
 14. Xiaoyue C, Qin Y, Shuangdi L, et al. Expression of the tumor suppressor miR-206 is associated with cellular proliferative inhibition and impairs invasion in ER α -positive endometrioid adenocarcinoma. *Cancer Lett.* 2012;314(1):41-53.
 15. Dai C, Xie Y, Zhuang X, Yuan Z. MiR-206 inhibits epithelial ovarian cancer cells growth and invasion via blocking c-met/AKT/mTOR signaling pathway. *Biomed Pharmacother.* 2018;104:763-770.
 16. Kuo YR, Jeng SF, Wang FS, Chen TH, Huang HC, Chang PR, Yang KD. Flashlamp pulsed dye laser (PDL) suppression of keloid proliferation through down-regulation of TGF-beta1 expression and extracellular matrix expression. *Lasers Surg Med.* 2004;34(2):104-108.
 17. Taro K, Ali Riza EE, Hiroaki N, Takashi H, Nobukazu H, Motohiro N. The flashlamp-pumped pulsed dye laser (585 nm) treatment of hypertrophic scars in Asians. *Ann Plast Surg.* 2003;51(4):366-371.
 18. Anderson RR, Parrish JA. Microvasculature can be selectively damaged using dye lasers: a basic theory and experimental evidence in human skin. *Lasers Surg Med.* 2010;1(3):263-276.
 19. Alster TS. Improvement of erythematous and hypertrophic scars by the 585-nm flashlamp-pumped pulsed dye laser. *Ann Plast Surg.* 1994;32(2):186-190.
 20. Alster TS, Williams CM. Treatment of keloid sternotomy scars with 585 nm flashlamp-pumped pulsed-dye laser. *Lancet.* 1995;345(8959):1198-1200.
 21. Adiel B, Tzipora G, Morse LS. Laser induces apoptosis and ceramide production in human retinal pigment epithelial cells. *Invest Ophthalmol Vis Sci.* 2005;46(7):2587.
 22. Yin K, Zhu R, Wang S, Zhao RC. Low level lasers effect on proliferation, migration and anti-apoptosis of mesenchymal stem cells. *Stem Cells Dev.* 2017;26(10):762-775.
 23. Shu B, Zhang LY, Li XP, Jiang WL, Zhang LQ. High-power helium-neon laser irradiation inhibits the growth of traumatic scars in vitro and in vivo. *Lasers Med Sci.* 2013;28(3):693-700.
 24. Salomon E, Isi E, Lev G, Juicheng H, Haydee B. Immunohistological evaluation of the healing response at the flap interface in patients with LASIK ectasia requiring penetrating keratoplasty. *J Refract Surg.* 2009;25(8):739.

How to cite this article: Zhang S, Zhao Z-M, Xue H-Y, Nie F-F. Effects of photoelectric therapy on proliferation and apoptosis of scar cells by regulating the expression of microRNA-206 and its related mechanisms. *Int Wound J.* 2020;17:317-325. <https://doi.org/10.1111/iwj.13272>